An Efficient Iris Recognition System using Phase-based Matching Technique

Shankargouda.M. Patil [1] , Sarojini B. K [2]

[1] Department of Electronics and Telecommunication, MBE society's College of Engineering Ambajogai 431517-INDIA
[2] Department of Electronics and Communication Engineering Basaveshwar Engineering College, Bagalkot-587102, INDIA

Abstract

A major approach for iris recognition today is to generate feature vectors corresponding to individual iris images and to perform iris matching based on some distance metrics. One of the difficult problems in feature-based iris recognition is that the matching performance is significantly influenced by many parameters in feature extraction process, which may vary depending on environmental factors of image acquisition. This paper presents an efficient algorithm for iris recognition using phase-based image matching. The use of phase components in 2D (two-dimensional) discrete Fourier transforms of iris images makes possible to achieve highly robust iris recognition in a unified fashion with a simple matching algorithm. Experimental evaluation using an iris image database clearly demonstrates an efficient matching performance of the proposed algorithm.

Keywords— Phase-based matching, Phase only correlation, Band limited phase-only correlation, Iris Recognition, image processing**.**

1. Introduction
1.1 Overview

Biometrics refers to the identification and verification of human identity based on certain physiological traits of a person. The commonly used biometric features include speech, fingerprint, face, handwriting, gait, hand geometry etc. The face and speech techniques have been used for over 25 years, while iris method is a newly emergent technique.

The iris is the colored part of the eye behind the eyelids, and in front of the lens. It is the only internal organ of the body which is normally externally visible. These visible patterns are unique to all individuals and it has been found that the probability of finding two individuals with identical iris patterns is almost zero. Though there lies a problem in capturing the image, the great pattern variability and the stability over time, makes this a reliable security recognition system.

1.2   Background

Ophthalmologists Alphonse Bertillon and Frank Burch were one among the first to propose that iris patterns can be used for identification systems. In 1992, John Daugman was the first to develop the iris identification software. Other important contribution was by R.Wildes et al. Their method differed in the process of iris code generation and also in the pattern matching technique. The Daugman system has been tested for a billion images and the failure rate has been found to be very low. His systems are patented by the *Iriscan Inc*. and are also being commercially used in Iridian technologies, UK National Physical Lab, British Telecom etc.

1.3   Organization of paper

This paper consists of six main parts, which are Introduction, image acquisition, preprocessing, Matching,; Simulation ,Results and discussions , Each section describes the theoretical approach and is followed by how it is implemented.

2. Image Acquisitions

This step is one of the most important and deciding factors for obtaining a good result. A good and clear image eliminates the process of noise removal and also helps in avoiding errors in calculation. In this case, computational errors are avoided due to absence of reflections, and because the images have been taken from close proximity. This project uses the image provided by CASIA (Institute of Automation, Chinese Academy of Sciences, http://www.sinobiometrics.com/) these images were taken solely for the purpose of iris recognition software research and implementation. Infra-red light was used for illuminating the eye, and hence they do not involve any specular reflections. Some part of the computation which involves removal of errors due to reflections in the image was hence not implemented.
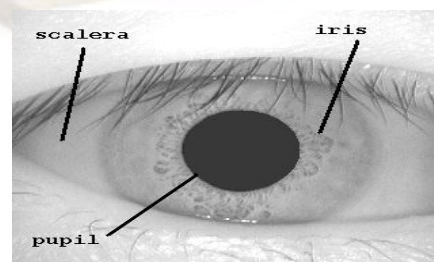

Figure 1: Image of the eye

3. Preprocessing
3.1 Image localization

Due to computational case, the image was scaled down by 60%. The image was filtered using Gaussian filter, which blurs the image and reduces effects due to noise. The degree of smoothening is decided by the standard deviation, σ and

The part of the eye carrying information is only the iris part. It lies between the scalera and the pupil. Hence the next step is separating the iris part from the eye image. The iris inner and outer boundaries are located by finding the edge image using the canny edge detector.

The Canny detector mainly involves three steps, viz. finding the gradient, non-maximum suppression and the hysteresis thresholding. As proposed by Wildes, the thresholding for the eye image is performed in a vertical direction only, so that the influence due to the eyelids can be reduced. This reduces the pixels on the circle boundary, but with the use of Hough transform, successful localization of the boundary can be obtained even with the absence of few pixels. It is also computationally faster since the boundary pixels are lesser for calculation.

Using the gradient image, the peaks are localized using non-maximum suppression. It works in the following manner. For a pixel imgrad(x,y), in the gradient image, and given the orientation theta(x,y), the edge intersects two of its 8 connected neighbors. The point at (x, y) is a maximum if its value is not smaller than the values at the two intersection points.

The next step, hysteresis thresholding, eliminates the weak edges below a low threshold, but not if they are connected to a edge above a high threshold through a chain of pixels all above the low threshold. In other words, the pixels above a threshold T1 are separated. Then, these points are marked as edge points only if all its surrounding pixels are greater than another threshold T2. The threshold values were found by trial and error, and were obtained as 0.2 and 0.19.

Hough transforms. Firstly, the threshold values are to be found by trial. Secondly, it is computationally intensive. This is improved by just having eight-way it is taken to be 2 in this case.

Figure 2: Canny edge image

Edge detection is followed by finding the boundaries of the iris and the pupil. Daugman proposed the use of the Integra-differential operator to detect the boundaries and the radii. It is given by

$$\max_{(r,x_0,y_0)} \left| G_\sigma(r) * \frac{\partial}{\partial r} \oint_{r,x_0,y_0} \frac{I(x,y)}{2\pi r} ds \right| \dots$$

......1

This behaves as a circular edge detector by searching the gradient image along the boundary of circles of increasing radii. From the likelihood of all circles, the maximum sum is calculated and is used to find the circle centers and radii.

The Hough transform is another way of detecting the parameters of geometric objects, and in this case, has been used to find the circles in the edge image. For every edge pixel, the points on the circles surrounding it at different radii are taken, and their weights are increased if they are edge points too, and these weights are added to the accumulator array. Thus, after all radii and edge pixels have been searched, the maximum from the accumulator array is used to find the center of the circle and its radius. The Hough transform is performed for the iris outer boundary using the whole image, and then is performed for the pupil only, instead of the whole eye, because the pupil is always inside the iris.

There are a few problems with symmetric points on the circle for every search point and radius. The eyelashes were separated by thresholding, and those pixels were marked as noisepixels,
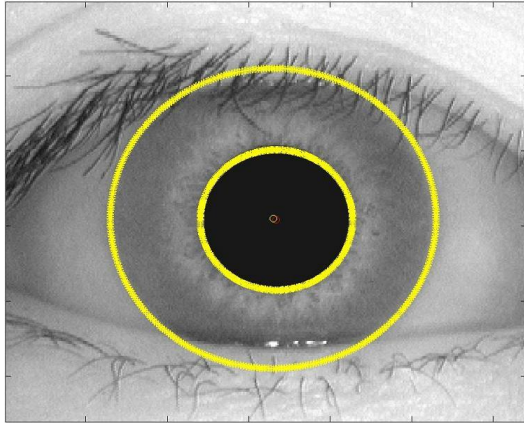
Figure 3: Image with boundaries

3.2 Image Normalization

Once the iris region is segmented, the next stage is to normalize this part, to enable generation of the iris templates' and their comparisons. Since variations in the eye, like optical size of the iris, position of pupil in the iris, and the iris orientation change person to person, it is required to normalize the iris image, so that the representation is common to all, with similar dimensions.

Normalization process involves unwrapping the iris and converting it into its polar equivalent. It is done using Daugman's Rubber sheet model. The center of the pupil is considered as the reference point and a remapping formula is used to convert the points on the Cartesian scale to the polar scale.

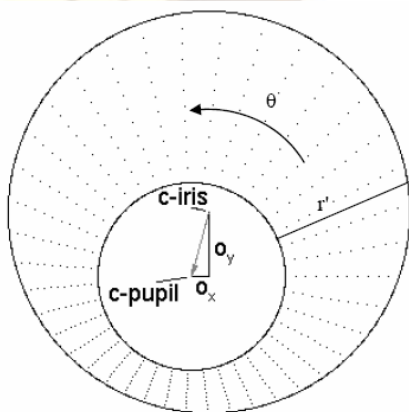The modified form of the model is shown bellow.

Figure 4: Normalization process

The radial resolution was set to 100 and the angular resolution to 2400 pixels. For every pixel in the iris, an equivalent position is found out on polar axes. The normalized image was then interpolated into the size of the original image, by using the interp2 function. The parts in the normalized image

which yield a NaN, are divided by the sum to get a normalized value.
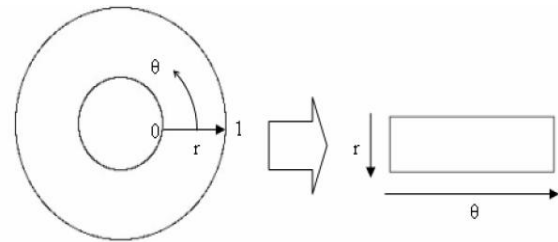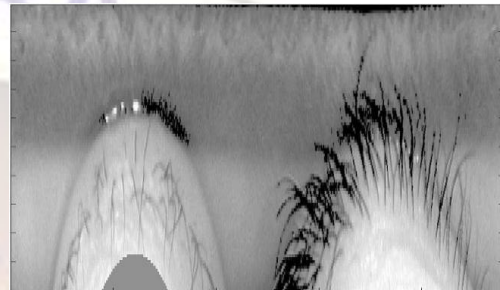

Figure 5: Unwrapping the iris

Figure 6: Normalized iris image

4. Matching

This method is performed to describe the detailed process of effective region extraction, image alignment, and matching score calculation. The main idea is to use the phase-based image matching for image alignment and matching score calculation.

4.1 Effective region extraction:

This step is performed to avoid certain problems, which occurs when the extracted effective region becomes too small to perform image matching. Given a pair of normalized iris images f $(n1, n2)$ and g $(n1, n2)$ to be compared, the purpose of this process is to extract from the two images, the effective regions f $(n1, n2)$ and g $(n1, n2)$ of same size, which do not contain irrelevant regions. The index range is assumed in any specified matrix where amplitude and phase is detected and evaluated. The inverse DFT is calculated. When two images are not similar, the peak drops and the height of the peak gives the good similarity measure for image matching and the localization of the peak shows the translation displacement of the image.

4.2 Phase-Based Image Matching:

Before discussing the image alignment and the matching score calculation, we introduce the principle of phase-based image matching using Phase-Only Correlation (POC) function [5].
Consider two $N1 \times N2$-pixel images, $f(n1, n2)$ and $g(n1, n2)$, where we assume that the index ranges are $n1 = -M1 \cdots M1$

($M1 > 0$) and $n2 = -M2 \cdots M2$ ($M2 > 0$) for mathematical simplicity, and hence $N1 = 2M1 + 1$ and $N2 = 2M2 + 1$. Let $F(k1, k2)$ and $G(k1, k2)$ denote the 2D DFTs of the two images. $F(k1, k2)$ is given by.
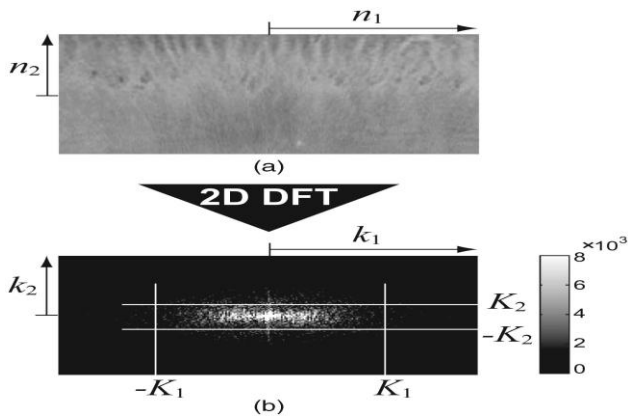

Figure 7: a) spatial domain b)frequency domain

$$F(k_1, k_2) = \sum_{n_1, n_2} f(n_1, n_2) W_{N_1}^{k_1 n_1} W_{N_2}^{k_2 n_2}$$
$$= A_F(k_1, k_2) e^{j\theta_F(k_1, k_2)}, \qquad ..2$$

The cross-phase spectrum $RFG(k1, k2)$ is given by

$$R_{FG}(k_1, k_2) = \frac{F(k_1, k_2)\overline{G(k_1, k_2)}}{|F(k_1, k_2)\overline{G(k_1, k_2)}|} = e^{j\theta(k_1, k_2)} \qquad \ldots\ldots3$$

The POC function $rfg(n1, n2)$ is the 2D Inverse DFT (2D IDFT) of $RFG(k1, k2)$ and is given by

$$r_{fg}(n_1, n_2) = \frac{1}{N_1 N_2} \sum_{k_1, k_2} R_{FG}(k_1, k_2) W_{N_1}^{-k_1 n_1} W_{N_2}^{-k_2 n_2} \qquad \ldots\ldots4$$

Band Limited phase only correlation (BLPOC)is given by

$$r_{fg}^{K_1 K_2}(n_1, n_2) = \frac{1}{L_1 L_2} \sum_{k_1, k_2}' R_{FG}(k_1, k_2) W_{L_1}^{-k_1 n_1} W_{L_2}^{-k_2 n} \qquad \ldots\ldots5$$

$n1 = -K1 \cdots K1$, $n2 = -K2 \cdots K2$, Note that the maximum value of the correlation peak of the BLPOC function is always normalized to 1 and does not depend on $L1$ and $L2$. Figure 5 shows an example of genuine matching using the original POC function. and the BLPOC function. The BLPOC function provides better discrimination capability than that of the original POC function.

4.2 Displacement alignment:

This step is performed to align the translational displacement between the extracted images. Various factors like rotation of camera; head tilt etc might cause displacement of the normalized images. The displacement parameter can be obtained as the peak location of the Phase only Correlation (POC) Function. The obtained parameters are used to align the images.

4.3 Matching score calculation:

Band limited phase only correlation is calculated in this step between the aligned images and evaluated the matching score. In the case of genuine matching, if the displacement between the two images is aligned, the correlation peak of BLPOC function should appear in the origin. If the matching score is close to the threshold value to separate genuine and imposters, we calculate the matching score with scale correction.(see figure 7)

5. Simulation:
Simulation model:

The proposed model has been simulated on a Pentium core2duo processor by using matlab 2009 programming language with image processing tool box for the performance and effectiveness of the approach.
The flow graph of our simulation work is as shown below figure 7.

Simulation Procedure:
Simulation procedure is as Explain bellow:
1) The matlab program saved in .m file.
2) File can be executed by using simulator tool in editor Window.
3) Add person's image to the data base.
4) Take one input image and performs pre-processing algorithm.
   a) To creates iris boundary.
   b) To creates pupil boundary.
   C) Normalized image.
5) Comparing input image with data base image.
6) If input image matches with data base image, "Matching is Successful".
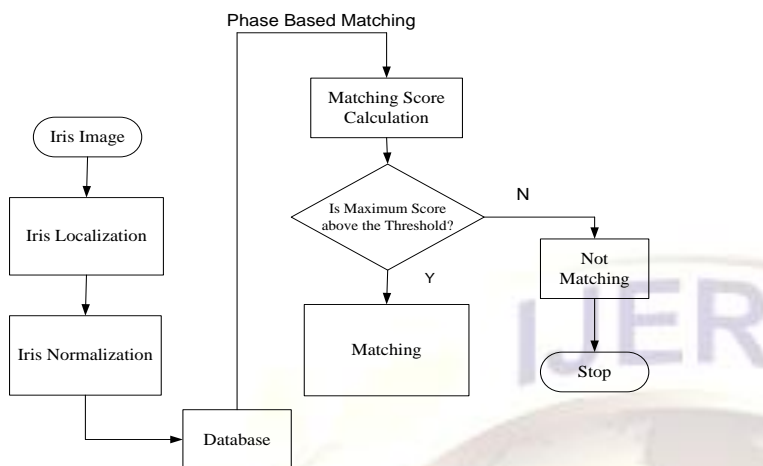7) Now calculate Phase only correlation function (POC).and BLPOC.

(B)

Phase Based Matching

Figure 7: process of flow diagram
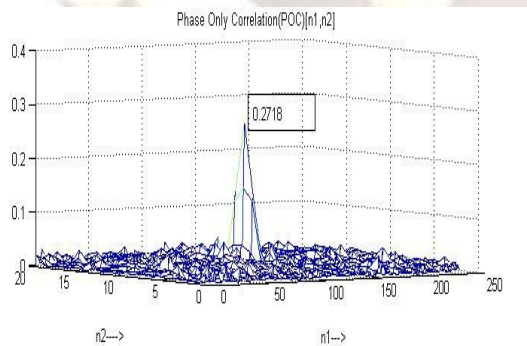
Algorithm:
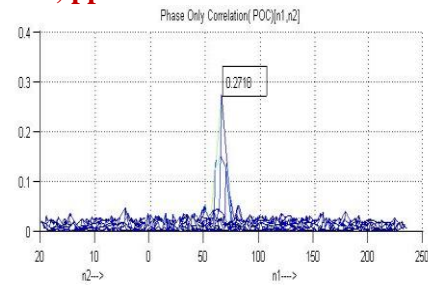**Begin:**

        Take input image.
        If   input image f
        F1=cong [fft (f)]
For all data base 20 people
    For all samples per person G1
        Matches F1 and G1
     POC   store to peak
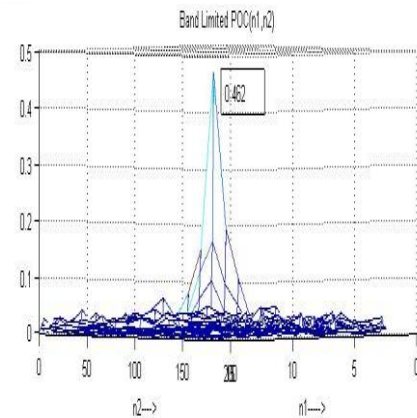   BLPOC   store to peak
     End
End

//TO find the maximum peak//
If   peak>Th   %Th= Threshold%
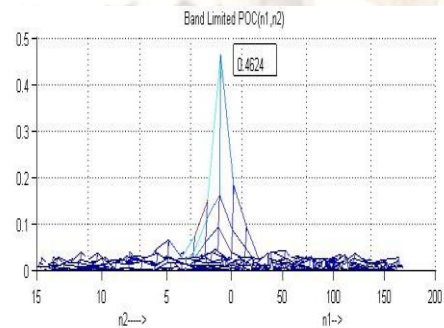   Match
Else
Not Match
End

(C)

(D)

Figure 8: Genuine matching using (A) & (B) The original POC Function and (C) & (D) The Band Limited POC function.
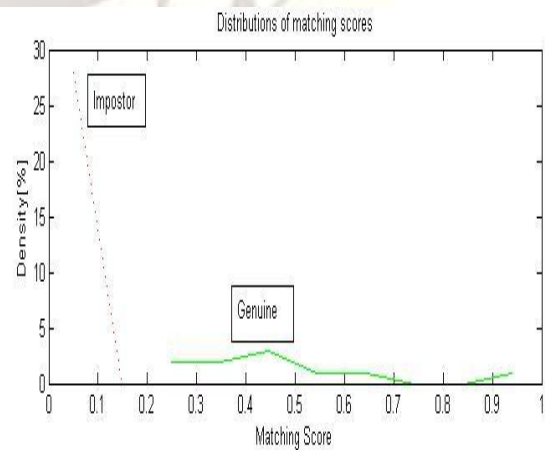

(A)

Figure 9: Distributions of matching score

6. Results and discussion:

This section describes a set of experiments using CASIA iris image database [6] for evaluating the proposed algorithm. This database contains 756 eye images (108 eyes and 7 images of each eye). We evaluate the genuine matching scores and the impostor matching scores for all the possible combinations (genuine: 2,268 attempts, impostor: 283,122 attempts).

The score between minimum genuine value and maximum impostor values can be chosen as a threshold.

Our observation shows that this performance degradation is mainly caused by the elimination of the eyelid masking and the effective region extraction steps. Note that CASIA iris image database contains many iris images whose irises are heavily occluded by eyelids. Thus, the eyelid masking and the effective region extraction steps have a significant impact on the performance. In a practical system, however, such a difficult condition does not happen so often. On the other hand, the processing time could be greatly reduced by the simplification which allows the system to perform multiple matching within a short time. This leads to better GAR (Genuine Accept Rate) for users. The number of iris images in the database available at [7] is smaller than the complete database. The result demonstrates a potential possibility of phase-based image matching for creating an efficient iris recognition system.

7. Conclusion:

The personal identification technique developed by John Daugman was implemented, with a few modifications involving due to processing speed. It has been tested only for the CASIA database image. Due to computational efficiency, the search area in a couple of parts has been reduced, and the elimination of errors due to reflections in the eye image has not been implemented.

8. Acknowledgment

References:

[1] J. Daugman, "High confidence visual recognition of persons by a test of statistical independence," *IEEE Trans. Pattern Analy. Machine Intell.*, vol. 15, no. 11, pp. 1148–1161, Nov. 1993.

[2] L. Ma, T. Tan, Y. Wang, and D. Zhang, "Efficient iris recognition by characterizing key local variations," *IEEE Trans. Image Processing*, vol. 13, no. 6, pp. 739–750, June 2004.

[3] B. Kumar, C. Xie, and J. Thornton, "Iris verification using correlation filters," *Proc. 4th Int. Conf. Audio- and Video-based Biometric Person Authentication*, pp. 697–705, 2003.

[4] K. Miyazawa, K. Ito, T. Aoki, K. Kobayashi, and H. Nakajima, "An efficient iris recognition algorithm using phase-based image matching," *Proc. Int. Conf. on Image Processing*, pp. II– 49–II–52, Sept. 2005.

[5] K. Miyazawa, K. Ito, T. Aoki, K. Kobayashi, and H. Nakajima, "A phase-based iris recognition algorithm," *Lecture Notes in Computer Science (ICB2006)*, vol. 3832, pp. 356–365, Jan. 2006.

[6] CASIA iris image database ver 1.0. http://www.sinobiometris.com

[7] K. Ito, H. Nakajima, K. Kobayashi, T. Aoki, and T. Higuchi, "A fingerprint matching algorithm using phase-only correlation," *IEICE Trans. Fundamentals*, vol. E87-A, no. 3, pp. 682–691, Mar. 2004.

[8] K. Ito, A. Morita, T. Aoki, T. Higuchi, H. Nakajima, and K. Kobayashi, "A fingerprint recognition algorithm combining phase-based image matching and feature-based matching," *Lecture Notes in Computer Science (ICB2006)*, vol. 3832, pp. 316–325, Jan. 2006.

[9] H. Nakajima, K. Kobayashi, M. Morikawa, K. Atsushi, K. Ito, T. Aoki, and T. Higuchi, "Fast and robust fingerprint identification algorithm and its application to residential access controller," *Lecture Notes in Computer Science (ICB2006)*, vol. 3832, pp. 326–333, Jan. 2006.

[10] Products using phase-based image matching. http://www.aoki.ecei.tohoku.ac.jp/poc/

[11] John Daugman, University of Cambridge, *How Iris Recognition Works*. Proceedings at International Conference on Image Processing.

[12] Tisse, Martin, Torres, Robert, *Personal Identification using human iris recognition,* Peter Kovesi, Matlab functions for Computer Vision and Image Processing